Nodal lines and nodal loops in nonsymmorphic odd-parity superconductors

T. Micklitz
Centro Brasileiro de Pesquisas Físicas, Rua Xavier Sigaud 150, 22290-180, Rio de Janeiro, Brazil

M. R. Norman
Materials Science Division, Argonne National Laboratory, Argonne, Illinois 60439, USA
(Received 29 October 2016; published 17 January 2017)

We discuss the nodal structure of odd-parity superconductors in the presence of nonsymmorphic crystal symmetries, both with and without spin-orbit coupling, and with and without time-reversal symmetry. We comment on the relation of our work to previous work in the literature, and also the implications for unconventional superconductors such as UPt_3.

DOI: 10.1103/PhysRevB.95.024508

I. INTRODUCTION

Power-law temperature dependences of certain physical properties in heavy electron superconductors that were discovered in the 1980s indicated the possible presence of nodes of the superconducting order parameter that form lines on the Fermi surface [1]. This motivated a study by Blount [2] where he showed that in the presence of spin-orbit coupling, one would not expect line nodes for an odd-parity order parameter: the constraint of having all three components of the triplet vanish can happen at most at points on the Fermi surface. This was an issue when an odd-parity order parameter was proposed to explain experimental data in UPt_3 [3,4] which was consistent with later phase sensitive Josephson tunneling measurements [5]. In 1995, though, one of the authors found a possible solution to this problem, by showing that there is a counterexample to Blount's theorem for nonsymmorphic odd-parity superconductors (UPt_3 being such an example given its $P6_3/mmc$ space group) [6]. By explicit construction of the pair wave functions, it was found that on the zone face, $k_z = \pi/c$, all components of the triplet belonged to the same group representation (as opposed to what happens on the $k_z = 0$ zone plane), meaning that for the proposed E_{2u} symmetry, line nodes are indeed possible (two of the Fermi surfaces of UPt_3 intersect this zone face). This was a consequence of the nonsymmorphic phase factors associated with the c axis (which is a screw axis for this space group). These considerations also potentially apply to other superconductors. For instance, UBe_{13} has the nonsymmorphic space group $Fm\bar{3}c$.

In 2009, a more rigorous treatment of this problem for the general nonsymmorphic case was formulated by us based on group theoretical arguments [7]. Very recently, this problem has been revisited by Yanase [8] and Kobayashi *et al.* [9]. The former found that the nodal "lines" actually reconstruct to form nodal "loops" (called "rings" in the latter) which, as we demonstrate here, shrink to zero as the ratio of the superconducting gap to the spin-orbit interaction increases. This is discussed in greater detail in Sec. III. The latter also discussed the mirror eigenvalues associated with these nodal loops, as well as contrasted the group theoretical and topological approaches to this problem. It is our purpose here to clarify matters by a general group theoretical approach that in addition generalizes our previous work to the case where spin-orbit interactions are absent, and also to the case of time-reversal symmetry breaking. We also consider the effect of glide-plane symmetries, and find that these do not protect line nodes as do the screw-axis symmetries.

II. GROUP THEORY

The nodal structure of superconducting order parameters can be understood from representations of the symmetry group of the underlying crystal. The absence of certain representations on high-symmetry planes or lines in the Brillouin zone implies the presence of line or point nodes of the Cooper-pair wave function, respectively, in cases where the Fermi surface intersects these planes or lines. Representations of the superconducting order parameter in symmorphic crystals are readily found from the underlying point-group symmetries [10]. Nonsymmorphic crystals, however, contain symmetries which consist of the combined operation of point-group elements with translations by fractions of a lattice vector. These nonprimitive translations generate additional phase factors which have to be accounted for in the derivation of the Cooper-pair representations. Indeed, these phase factors may conspire in a way to exclude some of the symmetry-allowed representations on high-symmetry planes, implying the possibility of new symmetry-enforced line nodes of the order parameter which are absent in symmorphic crystals [6,7]. A convenient way to derive space-group representations of the Cooper-pair wave function is to construct antisymmetrized products of the irreducible single-particle space-group representations [11–13], as we discuss next.

A. Induced Cooper-pair representations

Consider a centrosymmetric crystal generated by a nonsymmorphic space group. In the following, we denote space-group elements by $(g,\mathbf{t})$, where g refers to the point-group operation and $\mathbf{t}$ accounts for possible nonprimitive lattice translations, e.g., $(I,0)$ is the inversion symmetry, etc. Our focus here is on line nodes in odd-parity superconductors protected by nonsymmorphic symmetries. We therefore concentrate on odd-parity representations of the Cooper-pair wave function at Brillouin-zone points $\mathbf{k}$ belonging to symmetry planes of nonsymmorphic symmetry operations. Specifically, we consider symmetry planes $k_z = 0,\pi$ of a glide operation

$(\sigma_z,\mathbf{t}_\sigma)$ and the combined action of inversion and twofold screw axis, $(2_z,\mathbf{t}_2)(I,0)$ (from now on, we set the lattice constant to unity). Here and in the following, 2_z denotes the twofold rotation around the z axis, σ_z is reflection in the z plane, and $\mathbf{t}_{2/\sigma}$ is half a primitive translation along/perpendicular to the z direction.

One can construct representations of the Cooper-pair wave function from the single-particle representations $\gamma_\mathbf{k}$ of symmetry operations $m \in G_\mathbf{k}$ leaving $\mathbf{k}$ invariant (the "little group") [12]. To this end, one induces representations P^- of the antisymmetrized Kronecker product with vanishing total momentum (modulo a reciprocal lattice vector) [11–13]

$$\chi[P^-(m)] = \chi[\gamma_\mathbf{k}(m)]\chi[\gamma_\mathbf{k}(\mathcal{I}m\mathcal{I})], \tag{1}$$

$$\chi[P^-(\mathcal{I}m)] = -\chi[\gamma_\mathbf{k}(\mathcal{I}m\mathcal{I}m)], \tag{2}$$

where χ are the characters of the representation and for notational convenience we introduced $\mathcal{I} \equiv (I,0)$. In the presence of the spin-orbit interaction, the above equations characterize the pseudospin-triplet components of the Cooper-pair wave function. In the absence of spin-orbit, spin rotational symmetry is conserved and they account for the Cooper pair's orbital degree of freedom of a spin-triplet state.

Single-particle representations $\gamma_\mathbf{k}$ entering Eqs. (1) and (2) are double or single valued, depending on the presence of the spin-orbit interaction. Time-reversal symmetry θ can moreover induce extra degeneracies. These are detected by Herring's criterion [14,15] and taken into account by passing to the corresponding corepresentations (see Appendix A). We next apply the outlined procedure to construct Cooper-pair representations for the symmetries of interest.

B. Twofold screw axis

Consider first the presence of a twofold screw symmetry $(2_z,\mathbf{t}_2)$ along the z axis. Line nodes can be enforced on the symmetry planes $k_z = 0,\pi$ characterized by the little group $G_\mathbf{k} = \{(E,0),(\sigma_z,\mathbf{t}_2)\}$. Notice that in spite of its nonprimitive translation vector $(\sigma_z,\mathbf{t}_2) = (2_z,\mathbf{t}_2)\mathcal{I}$ is a symmorphic operation since the former can be removed by redefinition of the spatial origin (that is, it is a mirror plane, not a true glide plane). We next induce representations in the described manner, i.e., by defining characters for the symmetry operations in $G_\mathbf{k} \cup \mathcal{I}G_\mathbf{k} = \{(E,0),(\sigma_z,\mathbf{t}_2),(I,0),(2_z,\mathbf{t}_2)\}$.

Recalling the multiplication rule for nonsymmorphic group elements [12], $(g_1,\mathbf{t}_1)(g_2,\mathbf{t}_2) = (g_1g_2,\mathbf{t}_1 + g_1\mathbf{t}_2)$, it is verified that $\mathcal{I}(\sigma_z,\mathbf{t}_2)\mathcal{I} = e^{-ik_z}(\sigma_z,\mathbf{t}_2)$. We can thus simplify characters in Eqs. (1) and (2) for the symmetry planes of interest as summarized in Table I. From this table we then read off irreducible components of the Cooper-pair representations given in Table II. Notice that the second column in Tables I and II determines the mirror eigenvalue of the Cooper pair. We are thus left with the task of finding characters in the second and fourth columns which depend on the underlying symmetries.

TABLE I. Character table for representations P^- of antisymmetrized Kronecker deltas induced by single-particle representations of dimension d on the high-symmetry planes. For notational convenience, we suppress $\gamma_\mathbf{k}$.

	$(E,0)$	$(\sigma_z,\mathbf{t}_2)$	$(I,0)$	$(2_z,\mathbf{t}_2)$
$k_z = \pi$	d^2	$-\chi^2[(\sigma_z,\mathbf{t}_2)]$	$-d$	$\chi[(\sigma_z^2,0)]$
$k_z = 0$	d^2	$\chi^2[(\sigma_z,\mathbf{t}_2)]$	$-d$	$-\chi[(\sigma_z^2,0)]$

TABLE II. Character table for the irreducible representations of the Cooper-pair wave function on high-symmetry planes of a screw axis/glide plane ($\mathbf{t} = \mathbf{t}_{z/\sigma}$ for a screw axis/glide plane). The second column determines the mirror eigenvalue of the Cooper pair.

	$(E,0)$	$(\sigma_z,\mathbf{t})$	$(I,0)$	$(2_z,\mathbf{t})$
A_g	1	1	1	1
A_u	1	−1	−1	1
B_g	1	−1	1	−1
B_u	1	1	−1	−1

In the presence of the spin-orbit interaction, $\gamma_\mathbf{k}$ are double valued with purely imaginary eigenvalues. That is, $\chi[\gamma_\mathbf{k}(\sigma_z^2,0)] = -d$ and $\chi[\gamma_\mathbf{k}(\sigma_z,\mathbf{t}_2)] = \pm id$ with d the dimension of $\gamma_\mathbf{k}$. Time-reversal symmetry may induce extra degeneracies. Applying Herring's criterion, one indeed detects (Kramers) degeneracies on both symmetry planes. That is, $d = 2$ and one has to consider the corresponding double-valued corepresentations (see Appendix A for details). If time-reversal symmetry is broken, $\gamma_\mathbf{k}$ are one-dimensional. In the absence of the spin-orbit interaction, $\gamma_\mathbf{k}$ only account for the orbital degree of freedom, i.e., are single valued. That is, $\chi[\gamma_\mathbf{k}(\sigma_z^2,0)] = d$ and $\chi[\gamma_\mathbf{k}(\sigma_z,\mathbf{t}_2)] = \pm d$. Herring's criterion then signals degeneracies induced by time-reversal symmetry on the Brillouin-zone face $k_z = \pi$. The latter are known as "sticking of bands" induced by a twofold screw axis [14–16], and one has to pass to the single-valued corepresentation (see again Appendix A for details). When time-reversal symmetry is broken, $\gamma_\mathbf{k}$ are again one dimensional.

All characters of the induced representations are summarized in Appendix B. Table III gives the decomposition of the resulting Cooper-pair representations into irreducible components of Table II. The first four rows apply in the limit

TABLE III. Decompositions of Cooper-pair representations into their irreducible components. Here g and u denote the even- and odd-parity representations and A_g/B_u and B_g/A_u are representations which are even and odd under reflection in the symmetry plane (i.e., mirror eigenvalues ± 1), respectively. The results depend on the presence of time-reversal symmetry (TRS) and the spin-orbit (SO) interaction.

SO	TRS	BZ plane	Irreducible components
Yes	Yes	$k_z = \pi$	$P^- = A_g + 3B_u$
		$k_z = 0$	$P^- = A_g + B_u + 2A_u$
Yes	No	$k_z = \pi$	$P^- = B_u$
		$k_z = 0$	$P^- = A_u$
No	Yes	$k_z = \pi$	$P^- = A_g + B_u + 2A_u$
		$k_z = 0$	$P^- = B_u$
No	No	$k_z = \pi$	$P^- = A_u$
		$k_z = 0$	$P^- = B_u$

of a strong spin-orbit interaction. Following Anderson [17], analogs of Cooper-pair singlet and triplets can then be constructed from Kramers degenerate states $\mathbf{k},\theta I\mathbf{k}$ and their time-reversed partners $\theta\mathbf{k}, I\mathbf{k}$. The pseudospin singlet d_0 belongs to the one-dimensional even-parity representation (g) and the pseudospin-triplet states d_x,d_y,d_z span the three-dimensional odd-parity representation (u) [18]. On the high-symmetry planes, the representations are additionally characterized by their mirror eigenvalue, i.e., pair-wave functions are even (A_g,B_u) or odd (B_g,A_u) under reflection about the plane [19].

The first two rows show that transformation properties of pseudospin triplets with respect to the mirror plane change from the basal plane to the Brillouin zone face. That is, in the presence of time-reversal symmetry, all possible pair representations are allowed on the basal plane $k_z = 0$. This is in accordance with Blount's theorem, since d_x and d_y belong to one representation, and d_z to the other. On the Brillouin zone face, on the other hand, odd-parity representations which are odd under reflection in the plane are absent (that is, all components of $\mathbf{d}$ belong to the same representation). This opens the possibility of symmetry-protected line nodes when the Fermi surface intersects the Brillouin zone face and provides a counterexample to Blount's theorem as previously discussed in Refs. [6,7]. The third and fourth lines describe situations in which Kramers degeneracy is lifted by strong time-reversal symmetry breaking. In this case, only one of the four Cooper-pair functions survives, i.e., the pseudospin-triplet component formed from degenerate states $\mathbf{k}, I\mathbf{k}$ (we consider pairing of nondegenerate states later). Time-reversal symmetry breaking thus opens the possibility of symmetry-protected line nodes on both symmetry planes. This has also been discussed in a recent work by Nomoto and Ikeda [20].

The last four rows apply in the absence of the spin-orbit interaction. The indicated representations then classify the orbital part of the pair wave function. This is combined with one of the three symmetric spin-triplet states to guarantee overall antisymmetry of the pair wave function. In the absence of band degeneracies, representations are thus one dimensional, as in the last three rows, allowing for symmetry-protected line nodes on both symmetry planes. In the presence of time-reversal symmetry, the twofold screw axis induces, however, sticking of bands on the Brillouin zone face [14–16] (fifth row). One thus finds four allowed representations and both mirror eigenvalues are realized. In the absence of both the spin-orbit interaction and time-reversal breaking, symmetry-protected line nodes are thus possible on the basal plane but do not exist on the Brillouin-zone face. The difference from the first two lines of this table is that this sticking of bands allows the formation of interband pairs in this case [8]. The interband pairs are odd in the band index, implying that the intraorbital part of the Cooper-pair wave function is even to guarantee overall odd parity (that is, they have opposite mirror eigenvalues to the intraband pairs). We will return to this point below. In the absence of time-reversal symmetry, protected line nodes can appear on both symmetry planes, independent of the spin-orbit interaction. Finally, we note that for time-reversal symmetry breaking, the inversion of the sign of the Cooper-pair mirror eigenvalue of one-dimensional representations in the presence (third and fourth rows) and absence (seventh and eighth rows) of the spin-orbit interaction is readily related to the double and single valuedness of the representations.

TABLE IV. Character table for representations P^- of antisymmetrized Kronecker deltas induced by single-particle representations of dimension d on the high-symmetry planes. For notational convenience, we suppress $\gamma_{\mathbf{k}}$, and assume $\mathbf{t}_\sigma$ parallel to the x axis.

	$(E,0)$	$(\sigma_z,\mathbf{t}_\sigma)$	$(I,0)$	$(2_z,\mathbf{t}_\sigma)$
$k_z=\pi,0$	d^2	$e^{-ik_x}\chi^2[(\sigma_z,\mathbf{t}_\sigma)]$	$-d$	$-\chi\left[\left(\sigma_z^2,0\right)\right]$

C. Glide plane

Consider next a glide-plane symmetry $(\sigma_z,\mathbf{t}_\sigma)$, where without loss of generality we can assume $\mathbf{t}_\sigma$ parallel to the x axis. The little group on the symmetry planes $k_z = 0,\pi$ is $G_{\mathbf{k}} = \{(E,0),(\sigma_z,\mathbf{t}_\sigma)\}$ and we induce representations for the symmetry operations in $G_{\mathbf{k}} \cup \mathcal{I}G_{\mathbf{k}} = \{(E,0),(\sigma_z,\mathbf{t}_\sigma),(I,0),(2_z,\mathbf{t}_\sigma)\}$. Here $(2_z,\mathbf{t}_\sigma)$ in spite of its nonprimitive translation is a symmorphic operation (again the translation can be removed by redefinition of the spatial origin). Using the commutation relation $\mathcal{I}(\sigma_z,\mathbf{t}_\sigma)\mathcal{I} = e^{-ik_x}(\sigma_z,\mathbf{t}_\sigma)$, characters of the induced representations can be simplified, as shown in Table IV. The induced representations are identical on both symmetry planes. The dimension d and characters for $(\sigma_z,\mathbf{t}_\sigma)$ and $(\sigma_z^2,0)$ depend again on the underlying symmetries.

Let us first consider the presence of the spin-orbit interaction with double-valued representations, $\chi[\gamma_{\mathbf{k}}(\sigma_z^2,0)] = -d$. If time-reversal symmetry is preserved, Herring's criterion indicates the presence of (Kramers) degeneracies on both symmetry planes. That is, $d = 2$ and we need to pass to the double-valued corepresentation (see Appendix A for details). If time-reversal symmetry is broken, $\gamma_{\mathbf{k}}$ remain one dimensional and $\chi[\gamma_{\mathbf{k}}(\sigma_z,\mathbf{t}_\sigma)] = \pm ie^{ik_x/2}$. In the absence of the spin-orbit interaction, on the other hand, all single-particle representations are one dimensional, independent of time-reversal symmetry.

All characters of the induced representations are summarized in Appendix B. Table V shows the decompositions of the resulting Cooper-pair representations into irreducible components of Table II. If the spin-orbit interaction and time-reversal symmetry are both present, all odd-parity representations are allowed on both planes. That is, glide-plane symmetries do not provide us with counterexamples to Blount's theorem. In the absence of either time-reversal symmetry or the spin-orbit

TABLE V. Decompositions of Cooper-pair representations into their irreducible components. The latter depend on the presence of TRS and the SO interaction. Here, g/u denote representations which are even/odd under inversion and A_g/B_g, respectively, B_u/A_u which are even/odd under reflection in the symmetry plane.

SO	TRS	BZ plane	Irreducible components
Yes	Yes	$k_z=\pi,0$	$P^- = A_g + B_u + 2A_u$
Yes	No	$k_z=\pi,0$	$P^- = A_u$
No	Yes/no	$k_z=\pi,0$	$P^- = B_u$

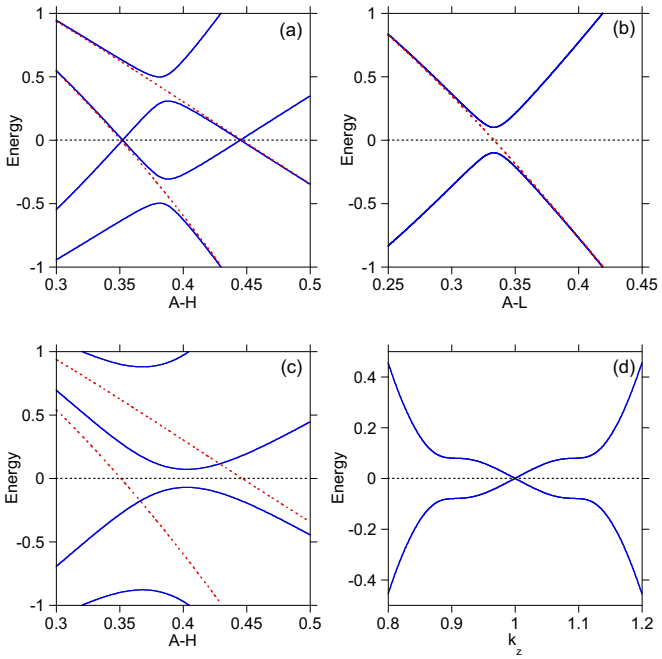

FIG. 1. Illustration of nodal loops in UPt_3 based on the toy model of Yanase [8]. Solid curves indicate the superconducting state dispersion, and dashed curves the normal state dispersion. (a) Dispersion along A-H for $\Delta = 0.1$, where A is $(0,0,\pi/c)$ and H is $(0,4/3a,\pi/c)$. (b) dispersion along A-L for $\Delta = 0.1$, where A is $(0,0,\pi/c)$ and L is $(2\pi/\sqrt{3}a,0,\pi/c)$. Here, Δ is the value of the superconducting E_{2u} order parameter in these energy units, this being the f function of Yanase which pairs electrons between two near-neighbor uranium sites (taken here as a constant for illustrative purposes). The nodes in (a) (due to the absence of intraband pairing for E_{2u} symmetry) and their lack thereof in (b) (due to interband pairing, which is allowed for this symmetry) lead to the two nodal lines closing to form nodal loops in the $k_z = \pi/c$ zone face. (c) Same as (a), but for $\Delta = 0.5$, showing the disappearance of the nodes along A-H, and thus the collapse of the nodal loops [23]. (d) dispersion along k_z normal to the second node along A-H in (a), illustrating that these are nodal loops, and not toroidal Fermi surfaces. This can also be seen from plots like in (a), where the nodes lift when k_z deviates from π/c.

interaction, symmetry-protected line nodes can occur on both symmetry planes.

Our discussion so far has shown that in the presence of time-reversal symmetry and the spin-orbit interaction, only twofold screw axes can protect line nodes in odd-parity superconductors. Next, we discuss that these line nodes typically form as loops.

III. NODAL STRUCTURE OF ODD-PARITY SUPERCONDUCTORS

As pointed out by Yanase [8], the nodal lines discussed above in the $k_z = \pi$ zone face actually reconstruct to form nodal loops in the case of UPt_3. The latter are, in contrast to line nodes, contractible, i.e., they continuously shrink to zero as the ratio of the superconducting gap to the spin-orbit interaction increases. The formation of these nodal loops can be understood from the results of Sec. II. In particular, along

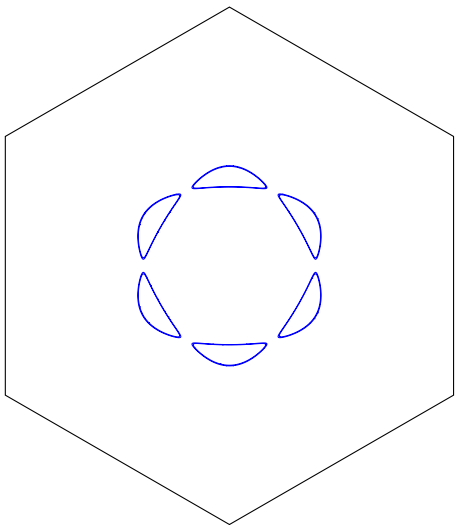

FIG. 2. Nodal loops in the $k_z = \pi/c$ zone face using the parameters from Fig. 1. They form due to the energy gap from interband pairing that occurs along the A-L lines.

the A-L lines of this zone face, the spin-orbit interaction vanishes, leading to band sticking (this band sticking effect has been seen in UPt_3 from breakdown orbits in de Haas–van Alphen measurements [21]). This means that interband pairs can form at these sticking points on the Fermi surface, and since they have opposite mirror eigenvalues, they are allowed representations for the case where the intraband pairs are not allowed. This leads to a gapping of the Fermi surface at these points, thus converting the nodal lines to nodal loops, as we illustrate in Figs. 1 and 2. As the order parameter increases, these nodal loops will eventually shrink to zero, leading to a topological transition [Fig. 1(c)]. In Ref. [9], topological arguments are presented (following earlier work [22]) that confirm the group theoretical ones. There, a claim was made that the topological arguments are more general than the group theory ones, but in fact they are equivalent. In particular, as we showed in Sec. II, in the presence of time-reversal symmetry breaking, the nodal structure of the pairs changes due to lifting of the degeneracy of the single-particle states.

Although much of the discussion above was motivated by UPt_3, there are other superconductors that have nonsymmorphic space groups. We earlier mentioned UBe_{13}. But its space group does not have a screw axis, but rather a glide plane, so we would not expect nodal lines in this case for odd-parity pairing, which is consistent with specific heat data [24]. But, URhGe, UCoGe, and UIr have screw axes, although the last breaks inversion symmetry, meaning even and odd parity can mix [1]. Moreover, the presence of magnetism can induce nonsymmorphic behavior and nodal lines as recently discussed in the context of UCoGe and UPd_2Al_3 [20]. Yet to be explored are the consequences of the effects discussed here on potential topological surface states. This will be addressed in future work.

ACKNOWLEDGMENTS

This work was supported by the Materials Sciences and Engineering Division, Basic Energy Sciences, Office of

Science, U.S. Department of Energy. T.M. acknowledges financial support by Brazilian agencies CNPq and FAPERJ.

APPENDIX A: HERRING'S CRITERION AND COREPRESENTATIONS

As stated in the main text, time-reversal symmetry θ can induce additional degeneracies. In this case, one should pass from the representations to corresponding corepresentations of the magnetic group $\mathcal{G}_{\mathbf{k}} = G_{\mathbf{k}} + \mathcal{I}\theta G_{\mathbf{k}}$. Degeneracies induced by θ can be detected by Herring's criterion from the sum of characters [15],

$$\sum_{B\in G_{\mathbf{k}}} \chi[\gamma_{\mathbf{k}}(\mathcal{I}\theta B)^2] = \begin{cases} +|G_{\mathbf{k}}|, & \text{case (a)} \\ -|G_{\mathbf{k}}|, & \text{case (b)} \\ 0, & \text{case (c).} \end{cases} \tag{A1}$$

Here $|G_{\mathbf{k}}|$ is the order of the little group. In case (a) no degeneracies are induced, while (b) and (c) indicate the presence of degeneracies. The latter are accounted for by passing to corepresentations $\gamma_{\mathbf{k}} \mapsto \Gamma_{\mathbf{k}} \equiv \begin{pmatrix} \gamma_{\mathbf{k}} & \\ & \bar{\gamma}_{\mathbf{k}} \end{pmatrix}$, where $\bar{\gamma}_{\mathbf{k}}(m) = \gamma_{\mathbf{k}}(m)$ in case (b) and $\bar{\gamma}_{\mathbf{k}}(m) = \gamma^*_{\mathbf{k}}[(\mathcal{I}\theta)^{-1} m\, \mathcal{I}\theta]$ in case (c), respectively, with "*" the complex conjugation. We next consider the cases of interest.

Twofold screw axis. In the presence of the spin-orbit interaction, the sum of characters for double-valued representations reads

$$\begin{aligned} &\chi([\mathcal{I}\theta(E,0)]^2) + \chi([\mathcal{I}\theta(\sigma_z,\mathbf{t}_2)]^2) \\ &\quad = -\chi[(E,0)] - e^{ik_z}\chi\left[\left(\sigma_z^2,0\right)\right] \\ &\quad = -1 + e^{ikz}, \end{aligned} \tag{A2}$$

where we used $\theta g_1 \theta g_2 = -g_1 g_2$. For double-valued corepresentations on the basal plane [case (c)], we then employ $\bar{\gamma}_{\mathbf{k}}[(\sigma_z,\mathbf{t}_2)] = \gamma^*_{\mathbf{k}}[(\mathcal{I}\theta)^{-1}(\sigma_z,\mathbf{t}_2)\mathcal{I}\theta] = \gamma^*_{\mathbf{k}}[(\sigma_z,\mathbf{t}_2)]$. For single-valued representations, on the other hand, $\theta g_1 \theta g_2 = g_1 g_2$ and

$$\begin{aligned} &\chi([\mathcal{I}\theta(E,0)]^2) + \chi([\mathcal{I}\theta(\sigma_z,\mathbf{t}_2)]^2) \\ &\quad = \chi[(E,0)] + e^{ik_z}\chi\left[\left(\sigma_z^2,0\right)\right] \\ &\quad = 1 + e^{ik_z}. \end{aligned} \tag{A3}$$

For the single-valued corepresentation on the Brillouin-zone face [case (c)], we use that $\bar{\gamma}_{\mathbf{k}}[(\sigma_z,\mathbf{t}_2)] = \gamma^*_{\mathbf{k}}((\mathcal{I}\theta)^{-1}(\sigma_z,\mathbf{t}_2)\mathcal{I}\theta) = -\gamma^*_{\mathbf{k}}((\sigma_z,\mathbf{t}_2))$.

Glide-plane symmetry. In the presence of the spin-orbit interaction

$$\begin{aligned} &\chi([\mathcal{I}\theta(E,0)]^2) + \chi([\mathcal{I}\theta(\sigma_z,\mathbf{t}_\sigma)]^2) \\ &\quad = -\chi[(E,0)] + \chi\left[\left(\sigma_z^2,0\right)\right] \\ &\quad = 0, \end{aligned} \tag{A4}$$

TABLE VI. Character table for representations P^- of antisymmetrized Kronecker deltas on symmetry planes induced by single-particle representations. Depending on the presence of TRS and the SO interaction, the latter are single or double-valued (co-) representations.

SO	TRS	BZ plane	$(E,0)$	$(\sigma_z,\mathbf{t}_2)$	$(I,0)$	$(2_z,\mathbf{t}_2)$
Yes	Yes	$k_z=\pi$	4	4	−2	−2
		$k_z=0$	4	0	−2	2
Yes	No	$k_z=\pi$	1	1	−1	−1
		$k_z=0$	1	−1	−1	1
No	Yes	$k_z=\pi$	4	0	−2	2
		$k_z=0$	1	1	−1	−1
No	No	$k_z=\pi$	1	−1	−1	1
		$k_z=0$	1	1	−1	−1

and for the double-valued corepresentations [case (c)], we then employ $\bar{\gamma}_{\mathbf{k}}[(\sigma_z,\mathbf{t}_\sigma)] = \gamma^*_{\mathbf{k}}[(\mathcal{I}\theta)^{-1}(\sigma_z,\mathbf{t}_z)\mathcal{I}\theta] = e^{ik_x}\gamma^*_{\mathbf{k}}[(\sigma_z,\mathbf{t}_2)]$, i.e., $\Gamma_{\mathbf{k}}[(\sigma_z,\mathbf{t}_\sigma)] = \pm e^{ik_x/2}\begin{pmatrix} & i \\ -i & \end{pmatrix}$. In the absence of the spin-orbit interaction

$$\begin{aligned} &\chi([\mathcal{I}\theta(E,0)]^2) + \chi([\mathcal{I}\theta(\sigma_z,\mathbf{t}_\sigma)]^2) \\ &\quad = \chi[(E,0)] + \chi\left[\left(\sigma_z^2,0\right)\right] \\ &\quad = 2. \end{aligned} \tag{A5}$$

APPENDIX B: IRREDUCIBLE REPRESENTATIONS OF THE COOPER-PAIR WAVE FUNCTION

We summarize the characters of induced representations in the case of a twofold screw axis (Table VI) and a glide-plane symmetry (Table VII). The decompositions of Cooper-pair representations into their irreducible components are done using the character table for the zero-momentum representations of the Cooper-pair wave function defined in Table II in the main text.

TABLE VII. Character table for representations P^- of antisymmetrized Kronecker deltas on symmetry planes induced by single- or double-valued (co-)representations.

SO	TRS	BZ plane	$(E,0)$	$(\sigma_z,\mathbf{t}_\sigma)$	$(I,0)$	$(2_z,\mathbf{t}_\sigma)$
Yes	Yes	$k_z=\pi,0$	4	0	−2	2
Yes	No	$k_z=\pi,0$	1	−1	−1	1
No	Yes/no	$k_z=\pi,0$	1	1	−1	−1

[1] C. Pfleiderer, Rev. Mod. Phys. **81**, 1551 (2009).
[2] E. I. Blount, Phys Rev. B **32**, 2935 (1985).
[3] J. A. Sauls, Adv. Phys. **43**, 113 (2004).
[4] M. R. Norman, Physica C **194**, 203 (2002).
[5] J. D. Strand, D. J. Van Harlingen, J. B. Kycia, and W. P. Halperin, Phys. Rev. Lett. **103**, 197002 (2009).
[6] M. R. Norman, Phys. Rev. B **52**, 15093 (1995).
[7] T. Micklitz and M. R. Norman, Phys. Rev. B **80**, 100506(R) (2009).
[8] Y. Yanase, Phys. Rev. B **94**, 174502 (2016).
[9] S. Kobayashi, Y. Yanase, and M. Sato, Phys. Rev. B **94**, 134512 (2016).
[10] G. E. Volovik and L. P. Gor'kov, Sov. Phys. JETP **61**, 843 (1985); K. Ueda and T. M. Rice, Phys. Rev. B **31**, 7114

(1985); M. Sigrist and K. Ueda, Rev. Mod. Phys. **63**, 239 (1991).
[11] C. J. Bradley and B. L. Davies, J. Math. Phys. **11**, 1536 (1970).
[12] C. J. Bradley and A. P. Cracknell, *The Mathematical Theory of Symmetry in Solids* (Oxford University Press, Oxford, 1972).
[13] V. G. Yarzhemsky, Phys. Status Solidi B **209**, 101 (1998); V. G. Yarzhemsky and E. N. Murav'ev, J. Phys.: Condens. Matter **4**, 3525 (1992).
[14] C. Herring, Phys. Rev **52**, 361 (1937).
[15] M. Lax, *Symmetry Principles in Solid State and Molecular Physics* (Wiley, New York, 1974).
[16] V. Heine, *Group Theory in Quantum Mechanics* (Dover, New York, 2007).
[17] P. W. Anderson, Phys. Rev. B **30**, 4000 (1984).
[18] The pseudospin singlet (corresponding to $S = 0$ in the absence of the spin-orbit interaction) is given by the even-parity combination $(\mathbf{k},\theta\mathbf{k}) - (\theta I\mathbf{k}, I\mathbf{k})$. The three pseudospin-triplet components (corresponding to $S = 1$ in the absence of the spin-orbit interaction) are given by the odd-parity combinations $(\mathbf{k}, I\mathbf{k})$, $(\theta I\mathbf{k},\theta\mathbf{k})$, and $(\mathbf{k},\theta\mathbf{k}) + (\theta I\mathbf{k}, I\mathbf{k})$. The latter are conveniently relabeled as a vector $\mathbf{d}$ and the above three states correspond to the components $-d_x + id_y$, $d_x + id_y$, and d_z, respectively.
[19] Our notation for A_u and B_u agrees with previous literature [25] that takes into account that $\mathbf{d}$ transforms as an axial vector.
[20] T. Nomoto and H. Ikeda, J. Phys. Soc. Jpn. **86**, 023703 (2017).
[21] G. J. McMullan, P. M. C. Rourke, M. R. Norman, A. D. Huxley, N. Doiron-Leyraud, J. Flouquet, G. G. Lonzarich, A. McCollam, and S. R. Julian, New J. Phys. **10**, 053029 (2008).
[22] S. Kobayashi, K. Shiozaki, Y. Tanaka, and M. Sato, Phys. Rev. B **90**, 024516 (2014).
[23] Calculations were done with the same parameters as in Ref. [8], that is, $t = 1$, $t_z = -4$, $t_p = 1$, $\alpha = 2$, and $\mu = 12$. The critical value of Δ for the nodal loop to disappear is given by $\Delta_{cr} = \sqrt{-\epsilon_+\epsilon_-}$ where $\epsilon_\pm = \epsilon_k \pm g_k$ with ϵ_k the normal state dispersion (without spin orbit), g_k the spin-orbit splitting, and k the value of the momentum at the dispersion minimum seen in (c).
[24] H. R. Ott, H. Rudigier, T. M. Rice, K. Ueda, Z. Fisk, and J. L. Smith, Phys. Rev. Lett. **52**, 1915 (1984).
[25] S. Yip and A. Garg, Phys. Rev. B **48**, 3304 (1993).